Tunneling of a heavy particle with spin in a metal

G. Zaránd
Institute of Physics, Technical University of Budapest, H 1521 Budafoki út 8, Budapest, Hungary
(Received 27 December 1994; revised manuscript received 24 May 1995)

The low-temperature behavior of a two-level system (TLS) with spin is investigated, where the atom tunneling between two positions possesses a spin and interacts with the conduction electrons by an exchange interaction. To describe the physical properties of this TLS a generalized model is developed, where in addition to the usual screening and electron assisted tunneling processes exchange interaction and exchange assisted interactions with the conduction electrons are introduced. These exchange interaction terms break the SU(2) symmetry of the original TLS model corresponding to the conduction-electron spin. Summing up the leading logarithmic vertex corrections we show that if the Kondo temperature associated with the orbital degrees of freedom, $T_K^{\rm orb}$, is smaller than that associated with the exchange interaction, $T_K^{\rm magn}$, then the orbital degrees of freedom of the TLS are frozen out when the magnetic Kondo effect takes place and only a magnetic Kondo effect occurs. In this case the ground state of the system seems to be a Fermi-liquid state. In the opposite case, $T_K^{\rm orb}>T_K^{\rm magn}$, two orbital electron channels become dominant below $T_K^{\rm orb}$ and a new fixed point appears. The possibility of experimental realizations is also shortly discussed.

I. INTRODUCTION

Two-level systems (TLS) play a very important role in the physics of disordered metallic samples,[1] nanostructures and point contacts.[2] TLS's can be the source of $1/f$ noise and time dependent conductance fluctuations,[3] but they can also give rise to logarithmic resistivity anomalies[4–8] and they provide a source of inelastic scattering mechanism for the phonons and the conduction electrons as well.[9,10]

A TLS can be formed by a heavy particle (impurity, some collective coordinate of a dislocation, heavy electron or a point defect) moving in a double-well potential. If the temperature is low enough then the higher excited states of the heavy particle (HP) are frozen out and the particle can move only by tunneling between the two nearly degenerate states associated with the two minima of the potential. Depending on the tunneling rate there may be two important processes due to the TLS-conduction electron interaction.

If the tunneling rate is small then the only important process is the screening of the conduction electrons (commutative case). This commutative TLS model has been studied intensively both theoretically[11–13] and experimentally[14,15] and it is already well understood. It is well known that the only important effect of screening is the renormalization of the tunneling rate of the HP as a function of temperature, and if the screening interaction is strong enough then it can result even in the localization of the HP in one minimum of the double-well potential.[12,13,16,17]

If the tunneling rate is large then assisted tunneling may also become important[5] (noncommutative case). In this process a conduction electron is scattered by the TLS while the HP is tunneling from one well to the other. In the noncommutative case a strongly correlated Kondo-like state is formed (orbital Kondo effect) with an energy, $T_K^{\rm orb}$, and logarithmic resistivity anomalies appear. The Kondo temperature $T_K^{\rm orb}$ is approximately given by[10]

$$T_K^{\rm orb}=D(v^x v^z)^{1/2}\left(\frac{v^x}{4v^z}\right)^{1/4v^z}, \tag{1.1}$$

where D is the bandwidth cutoff, and v^z and v^x denote the dimensionless couplings characteristic to screening and assisted tunneling, respectively. The couplings v^x and v^z in formula (1.1) denote some effective couplings, which take into account the strong renormalization of the bare matrix elements due to virtual hoppings to the excited states.[18] The prefactor $(v^x v^z)^{1/2}$ is obtained in the next to leading logarithmic approximation.

The nature of this strongly correlated state is still not completely clear. Recent experimental and theoretical investigations indicate[19–21] that well below the orbital Kondo temperature, $T_K^{\rm orb}$, the behavior of the noncommutative model is completely equivalent to that of the two-channel Kondo model exhibiting a non-Fermi-liquid behavior.[24,25] However, this conjecture has not been proved rigorously yet. It has been shown for the N_f-flavor TLS model,[21,22] that in the $1/N_f^2$ order the fixed point structure of this model is identical to that of the N_f-channel Kondo model.[23] However, in the TLS problem an infinite number of leading irrelevant operators appear even in the $1/N_f^2$ order, whose role in the low-temperature behavior is still unclear.

If the position of the HP is fixed then potential scattering plays no significant role, but an antiferromagnetic exchange interaction results in the formation of a magnetic Kondo state with energy

$$T_K^{\rm magn}=D(\rho_0 J)^{1/2}e^{-1/(2\rho_0 J)}, \tag{1.2}$$

where $\rho_0 J$ denotes the dimensionless exchange coupling.[26] This magnetic Kondo effect has been studied by a variety of techniques such as conformal field theory,[25] Bethe ansatz,[27] large N expansion,[28] and different renormalization group techniques,[16,29–33] and it is already well understood. It is well known that below the magnetic Kondo temperature, $T_K^{\rm magn}$, a spin compensation cloud is building up,[35] which at $T=0$, forms a singlet state with the impurity exhibiting Fermi-liquid behavior.[36,37] This can be contrasted to the orbital Kondo effect, where the ground state is believed to be

0163-1829/95/52(18)/13459(12)/$06.00

equivalent to that of the two-channel Kondo problem showing marginal Fermi-liquid properties.[24,25]

It is natural to ask what is going to happen if the HP has both magnetic and orbital degrees of freedom coupled to the conduction electrons. We shall see that if the HP moving in a double-well potential has a spin, then in addition to the screening and assisted tunneling other processes like "electron assisted exchange tunneling" appear. In this latter process a conduction electron is scattered by the TLS while the HP jumps from one position to the other with a spin flip. It will be shown that this process plays a very important role in the determination of the ground state properties of the TLS. It mixes the spin-up and spin-down electron channels like the particle-hole breaking term introduced by Pang *et al.* and may drive the system away from the non-Fermi-liquid fixed point.[33,34]

The interaction term derived turns out to have basically the same structure as the generalized Kondo model investigated by Cragg, Lloyd, and Nozières (CLN model).[38] Cragg *et al.* examined the interaction of a single localized d electron in a cubic environment, described by an Anderson Hamiltonian. In this case the crystal field lifts the fivefold orbital degeneracy of the d state and the ground state becomes — without considering spin degrees of freedom — doubly degenerate corresponding to the e_g irreducible representation of the cubic point group. Thus the localized electron has two different degrees of freedom: the real d-electron spin, and an orbital quantum number associated with the e_g representation. Then carrying out the Schrieffer-Wolff transformation one obtains an effective Kondo interaction term similar to the one given in Eq. (2.4).

However, there is an important difference between the two models. In the CLN model both the exchange and the orbital couplings are generated by the local Coulomb interaction and therefore, they are of the same order of magnitude. Thus, for physical model parameters one is always in the region $T_K^{\rm magn} > T_K^{\rm orb}$ and a single-channel Fermi-liquid fixed point is generated.[38,39] On the other hand, for a TLS with spin the ratio $T_K^{\rm orb}:T_K^{\rm magn}$ can be tuned by changing the geometry of the TLS or the conduction electron density of states, and both regions $T_K^{\rm magn} > T_K^{\rm orb}$ and $T_K^{\rm magn} < T_K^{\rm orb}$ are available. As we shall see in the case $T_K^{\rm orb} > T_K^{\rm magn}$ a different ground state appears.

To investigate the low-temperature dynamics of a tunneling particle with spin we apply the perturbative renormalization group approach.[29] The leading logarithmic scaling equations have already been constructed for the case of two orbital electron channels by Cragg *et al.*,[38] however, in this work no stability analysis has been carried out. In this paper we determine all the fixed points in the two-orbital-channel case for $T_K^{\rm magn} > T_K^{\rm orb}$ and we show that in this region only the Fermi-liquid fixed point is stable. We shall also present the results of numerical calculations for more than two channels which indicate that this Fermi-liquid fixed point is the stable one for any number of channels in the region, $T_K^{\rm magn} > T_K^{\rm orb}$. This result is in complete agreement with the results of Cragg *et al.* and Mirtschin *et al.*[38,39]

However, for $T_K^{\rm magn} < T_K^{\rm orb}$, the leading logarithmic equations indicate a completely different behavior of the model. As we shall see, due to the orbital Kondo effect two orbital electron channels become dominant, and a new ground state seems to appear, where magnetic and orbital correlations play equally important roles.

The paper is organized as follows: In Sec. II we describe the model introduced to describe a tunneling HP with spin and we derive the scaling equations. In Sec. III we study the solution of the scaling equations in the special case where only a single orbital channel is considered. In Sec. IV we examine the fixed point structure of the scaling equations for several orbital conduction electron channels. Our concluding remarks and the discussion of the possible experimental realizations are given in Sec. V. Some technical details of the calculations can be found in the Appendices.

II. MODEL HAMILTONIAN

In this section we shortly derive the model Hamiltonian used to describe the dynamics of the tunneling spin and we derive the leading order scaling equations. Our Hamiltonian consists of three terms.

The first term describes the motion of the HP in the double-well potential. As we have already noted in the Introduction if the temperature is low enough (i.e., if it is much smaller than the Debye temperature) then the motion of the HP is mainly restricted to the lowest lying two states associated with the two minima of the potential. In this case the orbital motion of the HP can be described by a one-half orbital pseudospin τ, the states $\tau^3 = \pm 1$ corresponding to the left- and right-hand-side states of the potential. The Hamiltonian of the TLS can be written as

$$H_h = \frac{1}{2}\sum_{i,\alpha,\beta,s} \Delta_i (b^+_{\alpha s}\tau^i_{\alpha\beta} b_{\beta s}), \tag{2.1}$$

where the τ^i's $(i=1,\ldots,3)$ are the Pauli matrices, $\alpha,\beta = \pm 1$ are the orbital pseudospin of the TLS and $s = -S,\ldots,S$ denotes the z component of the spin of the HP. The pseudofermion creation and annihilation operators, $b^+_{\alpha s}$ and $b_{\alpha s}$, respectively, are introduced for technical purposes.[40] Writing the Hamiltonian in the form (2.1) we neglected the spin-orbit interaction, therefore, the HP term (2.1) is diagonal in the spin s of the HP. The lowest lying $2(2S+1)$ states of the HP are not completely degenerate due to the eventual asymmetry of the potential and the tunneling through the barrier. However, if the temperature is much larger than the splitting $\Delta = (\Sigma_i \Delta_i^2)^{1/2}$ of these states then the ground states of the tunneling center can be considered as $2(2S+1)$ times degenerate. In this paper we only consider the temperature range where $T \gg \Delta$, and therefore, the ground state of the TLS is taken to be $2(2S+1)$ times degenerate. In the opposite case, $T \ll \Delta$, the state of the HP is only $2S+1$ times degenerate corresponding to the spin degrees of freedom of the HP and the physics of the simple Kondo model is recovered.

The second term of the Hamiltonian describes the band of the conduction electrons

$$H_{\rm el} = \sum_{\mathbf{k},\sigma} \epsilon(\mathbf{k}) a^+_{\mathbf{k}\sigma} a_{\mathbf{k}\sigma}, \tag{2.2}$$

where $\sigma = \pm 1$ is the conduction electron spin and $\epsilon(\mathbf{k})$ denotes the energy of a conduction electron with momentum

$\mathbf{k}$ measured from the Fermi energy. The $a^+_{\mathbf{k}\sigma}$'s ($a_{\mathbf{k}\sigma}$'s) are creation (annihilation) operators of a conduction electron with momentum $\mathbf{k}$ and spin σ. Throughout this paper we assume that the density of states of the conduction electrons for one spin direction, $\rho(\epsilon)$, is uniform between the high and low energy cutoffs D and $-D$, respectively: $\rho(\epsilon)=\rho_0$. This simplification does not influence the universal features of the low-temperature behavior of the model but makes the calculation much simpler.

Finally, the third term of the Hamiltonian describes the TLS-electron interaction. For the sake of simplicity we assume that the interaction between the conduction electrons and the tunneling spin can be described by a pseudopotential and an exchange interaction term depending only on the relative position of the HP and the conduction electrons

$$H_{\rm int}=\sum_j \left\{ U(\mathbf{r}_j-\mathbf{R})+J(\mathbf{r}_j-\mathbf{R})\sum_{i=1}^{3}\sigma^i(j)S^i \right\}, \quad (2.3)$$

where $\sigma(j)$ and $\mathbf{r}_j$ denote the spin and the coordinate of the jth conduction electron, and $\mathbf{R}$ is the coordinate of the HP. For this simple effective interaction the second quantized expression of the interaction term becomes

$$H_{\rm int}=\frac{1}{N}\sum_{i,s,\mathbf{k},\mathbf{k}',\sigma} U^{\mu}_{\mathbf{k}\mathbf{k}'} b^+_{\alpha s}\tau^{\mu}_{\alpha\alpha'} b_{\alpha' s} a^+_{\mathbf{k}\sigma}a_{\mathbf{k}'\sigma} + \frac{1}{N}\sum_{\substack{i,\mu,s,s',\mathbf{k}\\ \mathbf{k}',\sigma,\sigma'}} J^{\mu}_{\mathbf{k}\mathbf{k}'} b^+_{\alpha s}\tau^{\mu}_{\alpha\alpha'} S^i_{ss'} b_{\alpha' s'}(a^+_{\mathbf{k}\sigma}\sigma^i_{\sigma\sigma'}a_{\mathbf{k}'\sigma'}). \quad (2.4)$$

In Eq. (2.4) the index μ takes the values $\mu=\{0,\ldots,3\}$ N is the number of unit cells in the sample, and we have introduced the unit matrix $\tau^0_{\alpha\beta}=\delta_{\alpha\beta}$. The coupling constants $J^{\mu}_{\mathbf{k}\mathbf{k}'}$ and $U^{\mu}_{\mathbf{k}\mathbf{k}'}$ can be expressed in terms of the effective interactions $J(\mathbf{r}-\mathbf{R})$ and $U(\mathbf{r}-\mathbf{R})$ as simple integrals

$$J^{\mu}_{\mathbf{k}\mathbf{k}'}=\frac{N}{2}\sum_{\alpha,\beta}\tau^{\mu}_{\beta\alpha}\int d^3\mathbf{r}\int d^3\mathbf{R}\varphi^*_{\mathbf{k}}(\mathbf{r})\varphi_{\mathbf{k}'}(\mathbf{r})J(\mathbf{r}-\mathbf{R}) \times\Psi^*_{\alpha}(\mathbf{R})\Psi_{\beta}(\mathbf{R}),$$

$$U^{\mu}_{\mathbf{k}\mathbf{k}'}=\frac{N}{2}\sum_{\alpha,\beta}\tau^{\mu}_{\beta\alpha}\int d^3\mathbf{r}\int d^3\mathbf{R}\varphi^*_{\mathbf{k}}(\mathbf{r})\varphi_{\mathbf{k}'}(\mathbf{r})U(\mathbf{r}-\mathbf{R}) \times\Psi^*_{\alpha}(\mathbf{R})\Psi_{\beta}(\mathbf{R}). \quad (2.5)$$

Here the $\varphi_{\mathbf{k}}$'s denote the spin independent part of the wave functions of the conduction electrons while Ψ_{α} ($\alpha=\pm1$) are the states of the HP associated with the two minima of the potential well. Similarly to the TLS problem[10] a simple estimation of the amplitude of the integrals in (2.5) gives that for a realistic TLS $|J^0|\gg|J^3|\gg|J^1|\sim|J^2|$.

Constructing the Hamiltonian above we restricted the motion of the HP artificially to the two lowest lying eigenstates of the double-well potential. In the reality the higher excited states of the HP are also mixed into the strongly correlated Kondo state due to the virtual assisted hopping processes.[18] Similarly to the case of a simple TLS (Ref. 18) these assisted hoppings can strongly renormalize the couplings appearing in Eq. (2.4) and they can modify the Kondo temperature by 1 or 2 orders of magnitude. However, the low-temperature properties of the system, the critical exponents and the structure of the ground state remain essentially unchanged. Therefore we do not consider here the contribution of the higher excited states.

The interaction part of the Hamiltonian is rather complex. The first part of it, the potential scattering part, describes "simple" assisted tunneling and screening interactions mentioned in the Introduction. The second spin dependent part of the interaction term corresponds to "exchange screening" and "exchange assisted tunnelings." The latter can be interpreted as a tunneling process due to the electronic spin density fluctuations at the potential barrier, and the interpretation of the "exchange screening" is also very similar to that of the "potential screening" v^z in Eq. (1.1).

To simplify the problem one usually introduces a new set of dimensionless coupling constants by means of a complete orthogonal set of functions at the Fermi surface, $\{f_n(\mathbf{k})\}$:

$$A_{\mathbf{k}\mathbf{k}'}\rightarrow a_{nn'}=\rho_0\int\frac{dS_{\mathbf{k}}}{S_F}\frac{dS_{\mathbf{k}'}}{S_F}f^*_n(\mathbf{k})A_{\mathbf{k}\mathbf{k}'}f_{n'}(\mathbf{k}'), \quad (2.6)$$

where $A_{\mathbf{k}\mathbf{k}'}$ refers to the couplings $J^{\mu}_{\mathbf{k}\mathbf{k}'}$ and $U^{\mu}_{\mathbf{k}\mathbf{k}'}$, while $a_{nn'}$ stands for the dimensionless couplings $(j_{\mu})_{nn'}$ and $(u_{\mu})_{nn'}$. The integration is carried out at the Fermi surface, $dS_{\mathbf{k}}$ and S_F being the surface element and the total area of the Fermi surface, respectively. The index n denotes the orbital quantum number of the conduction electrons. The choice of the functions $\{f_n(\mathbf{k})\}$ is not unique; they can be chosen according to the actual shape of the Fermi surface, to the nature of the atomic orbitals or to the crystal field symmetry as well.

The leading order scaling equations can be generated in the standard way from the second-order logarithmic vertex corrections by reducing the high energy cutoff D. Carrying out the calculation one finally obtains

$$\frac{d\underline{u}_0}{dx}=0, \quad (2.7)$$

$$\frac{d\underline{u}_{\mu}}{dx}=-i\sum_{\nu,\rho=1}^{3}\epsilon^{\mu\nu\rho}([\underline{u}_{\nu},\underline{u}_{\rho}]+S(S+1)[\underline{j}_{\nu},\underline{j}_{\rho}]) \quad (\mu=1,2,3), \quad (2.8)$$

$$\frac{d\underline{j}_0}{dx}=2\sum_{\mu=0}^{3}\underline{j}_{\mu}\underline{j}_{\mu}, \quad (2.9)$$

$$\frac{d\underline{j}_{\mu}}{dx}=2\{\underline{j}_0,\underline{j}_{\mu}\}-i\sum_{\nu,\rho=1}^{3}\epsilon^{\mu\nu\rho}([\underline{u}_{\nu},\underline{j}_{\rho}]+[\underline{j}_{\nu},\underline{u}_{\rho}]) \quad (\mu=1,2,3), \quad (2.10)$$

where we have introduced the matrix notation $(j_{\mu})_{nm}\rightarrow\underline{j}_{\mu}$ and $(u_{\mu})_{nm}\rightarrow\underline{u}_{\mu}$, and the scaling parameter x denotes $x=\ln(D_0/D)$, D_0 being the initial value of the high energy

cutoff. The symbols [,] and {,} stand for the commutators and anticommutators, respectively, and $\epsilon^{\mu\nu\rho}$ denotes the Levi-Civita symbol.

Concerning these scaling equations we have to note that the simple potential scattering amplitude $\underline{u}_0$ remains unscaled as expected, while the scaling equations of the other couplings are coupled to each other. This suggests that the magnetic Kondo effect can generate orbital correlations in the ground state, and similarly, the orbital correlations due to the orbital Kondo effect are able to generate magnetic correlations at the same time. On the other hand, the scaling equations are rather asymmetrical with respect to the couplings $\underline{u}_\mu$ and $\underline{j}_\mu$. This indicates that — depending on the ratio of the energy scales $T_K^{\rm orb}$ and $T_K^{\rm magn}$ — there may be a transition in the structure of the stable fixed point approached by the system.

III. THE CASE OF ONE ORBITAL CHANNEL

To gain insight to the nature of the ground state of the Hamiltonian it is instructive to consider the case of a single orbital conduction electron channel. Since the s-wave conduction electrons are scattered much more effectively by the TLS than the others, one could think that dropping all the higher angular momentum channels is a reasonable approximation. As we shall see in the next section for $T_K^{\rm magn} > T_K^{\rm orb}$ this approximation works quite well and the ground state of the system is very similar to the one found in this section.

In the case of a single orbital channel the matrices $\underline{j}_\mu$ and $\underline{u}_\mu$ are replaced by simple scalar couplings, j_μ and u_μ. Therefore, all the commutators vanish in Eqs. (2.8) and the scaling equations can be integrated exactly.

For the sake of simplicity we consider a symmetrical double-well potential. In this case symmetry implies that the couplings j_2 and j_3 vanish and only two relevant coupling constants remain: j_0 and j_1. As it is shown in Appendix A even in this oversimplified case the initial coupling j_1 does not vanish and leads to the appearance of a nontrivial solution of the scaling equations.

Since the potential scattering amplitudes are unscaled only Eqs. (2.9) and (2.10) are relevant:

$$\frac{dj_0}{dx} = 2(j_0^2 + j_1^2), \tag{3.1}$$

$$\frac{dj_1}{dx} = 4 j_0 j_1. \tag{3.2}$$

These scaling equations can be integrated easily and one obtains that the scaling trajectories are determined by the following equation:

$$\frac{j_1}{j_0^2 - j_1^2} = \frac{j_1(0)}{j_0(0)^2 - j_1(0)^2} \equiv \frac{1}{a}, \tag{3.3}$$

where $j_0(0)$ and $j_1(0)$ denote the initial values of the couplings j_0 and j_1. The scaling trajectories of j_0 and j_1 are shown in Fig. 1 for different values of the parameter a defined in Eq. (3.3).

For ferromagnetic exchange coupling ($j_0 < 0$), theoretically, two different situations may arise. If $|j_0| > |j_1|$ then

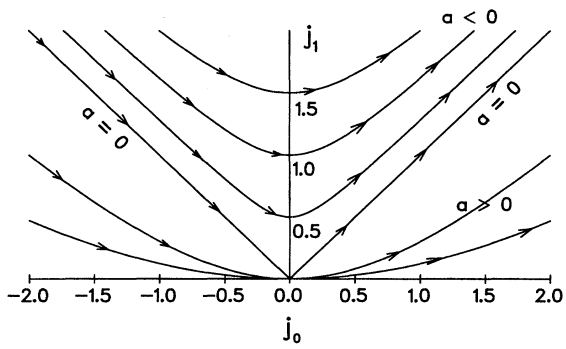

FIG. 1. The scaling trajectories of the couplings j_1 and j_0 in the case of a single orbital channel. The $j_0 = 0$ axis (indicated by a heavy line) is marginally stable and the $j_1 = 0$ trajectory corresponding to the usual Kondo trajectory is unstable.

both j_1 and j_0 tend to zero as $T \to 0$, i.e., the interaction is irrelevant in the $T \to 0$ limit. In the opposite case $|j_0| < |j_1|$, however, both j_0 and j_1 scale to infinity as the bandwidth scales to zero, $x \to \infty$. Thus, unlike the ferromagnetic Kondo Hamiltonian in this case the spin flip scattering of the conduction electrons may be relevant as $T \to 0$ and the amplitude of assisted exchange tunneling diverges at zero temperature. However, in the physical situation only the case $|j_0| > |j_1|$ can occur since $j_1 \sim (k_F d)^2 j_0$, where k_F denotes the Fermi momentum of the conduction electrons and d is the distance between the two minima of the double well potential (see Appendix A). Therefore, we can conclude that for ferromagnetic coupling the exchange interaction is irrelevant. We stress at this point that the physical values of the initial couplings for the TLS case differ essentially from those of the Kondo problem.[38] While for the Kondo model $|j_1| > |j_0|$, i.e., the model always scales to strong coupling, for the TLS with spin the opposite case, $|j_1| < |j_0|$, occurs and the exchange interaction becomes irrelevant in the ferromagnetic case.

In the antiferromagnetic case, $j_0 > 0$, similarly to the ordinary Kondo problem, both the couplings j_1 and j_0 diverge as $\sim [\ln(D_0/T_K)]^{-1}$, where the leading logarithmic Kondo temperature T_K is determined by the largest of the two couplings $j^{\pm} = j_0 \pm j_1$:

$$T_K = D_0 \exp\{-1/2 \max(j^+, j^-)\}. \tag{3.4}$$

As can be seen in Fig. 1 the conventional Kondo trajectory corresponding to the axis $j_1 = 0$ is unstable.

In the antiferromagnetic case in the $x \to \infty$ limit the asymptotic values of the couplings j_1 and j_0 are related by the relation $j_0 \approx j_1 + a/2$. Then using the simple estimates of Appendix A the divergent part of the effective Hamiltonian becomes

$$H_{\rm int}^{\rm eff}(x) = 2D_0 \frac{1}{N} \sum_{i,s,s',\epsilon,\epsilon',\sigma} j_0(x) [b_s^+ (1 - \tau^1) b_{s'}] \times S^i_{ss'} a^+_{\epsilon\sigma} \sigma^i_{\sigma\sigma'} a_{\epsilon'\sigma'}, \tag{3.5}$$

where the orbital quantum numbers of the TLS were suppressed, and the energies ϵ and ϵ' of the conduction elec-

trons fall into the interval $(-D,D)$. This interaction term tells us that the conduction electrons are interacting with the TLS only if it is in the state $\tau^1=-1$. Therefore, as soon as the Kondo-like ground state is formed the degeneracy of the states $\tau^1=\pm 1$ will be split, and the motion of the HP is expected to be frozen out. As we shall see in Sec. IV for $T_K^{\rm magn}>T_K^{\rm orb}$ this is also the case if more orbital channels are considered and the magnetic Kondo effect results in the "localization" of the HP. It is important to note that this localization does not occur in coordinate space, but according to Eq. (3.5) the HP prefers freezing into the antisymmetric state, $\tau^1=-1$.

Since for a physical system $j_0 \gg j_1$, the Kondo effect is driven by the exchange coupling j_0. Therefore, the Kondo temperature T_K is approximately the same as it would be for a localized spin in the same material. However, as the coupling j_0 starts to increase the initially negligible coupling j_1 is generated, and finally the ground state becomes very much different from the one corresponding to the couplings $j_0 \to \infty$ and $j_1=0$, which would be naively expected to occur.

IV. THE CASE OF TWO AND MORE CHANNELS

In this section we analyze the asymptotic behavior ("fixed point structure") of the scaling equations in the antiferromagnetic case for two and more orbital channels and we investigate analytically the symmetry structure of the strongly correlated state formed. The fixed point structure of the Hamiltonian, Eq. (2.4), has already been analyzed by Cragg *et al.* using the numerical renormalization group (NRG) technique. However, because of computational limitations they could only examine the case of two conduction electron orbital channels. Furthermore, they have not explored the case $T_K^{\rm orb}>T_K^{\rm magn}$. Our calculations indicate that in this latter case a Kondo state is formed, which is different from the $T_K^{\rm orb}<T_K^{\rm magn}$ ground state examined by Cragg *et al.*[38] We first consider the case $T_K^{\rm magn}>T_K^{\rm orb}$ in detail. The opposite case, $T_K^{\rm magn}<T_K^{\rm orb}$, will be discussed at the end of this section.

Since in the case, $T_K^{\rm magn}>T_K^{\rm orb}$, the couplings $\underline{u}_\mu$ are generated by the $\underline{j}_\mu$'s appearing on the right-hand side of Eq. (2.8), we first investigate the asymptotic behavior of the $\underline{j}_\mu$'s by dropping the second term in Eq. (2.10). The correctness of this approximation will be justified later.

We look for the asymptotic solution of the scaling equations in the form

$$\underline{j}_\mu=\hat{\underline{j}}_\mu f, \tag{4.1}$$

where the function $f(x)=1/[2(x_c-x)]$ satisfies the differential equation $f'=2f^2$, x_c being the critical value of the scaling variable corresponding to the Kondo temperature, $x_c=\ln(D_0/T_K)$. For a general scaling trajectory the couplings $\hat{\underline{j}}_\mu$ defined in Eq. (4.1) depend on the scaling parameter x. A "fixed point" of the scaling equations is determined by the condition that the $\hat{\underline{j}}_\mu$'s be independent of x. In this case the matrix coefficients $\hat{\underline{j}}_\mu$ must satisfy the following algebraic equations:

$$\hat{\underline{j}}_0=\sum_{\mu=0}^{3}\hat{\underline{j}}_\mu\hat{\underline{j}}_\mu, \quad \hat{\underline{j}}_\mu=\{\hat{\underline{j}}_\mu,\hat{\underline{j}}_0\} \quad (\mu=1,2,3). \tag{4.2}$$

These equations cannot be solved in the general case, but in the case of two orbital channels one can determine their solutions exactly.

For two orbital channels the couplings $\hat{\underline{j}}_\mu$ and $\underline{j}_\mu$ can be expanded in terms of the Pauli matrices ρ^a $(a=0,1,2,3)$:

$$\hat{\underline{j}}_\mu=\sum_{a=0}^{3}\hat{j}_{\mu a}\rho^a, \quad \underline{j}_\mu=\sum_{a=0}^{3}j_{\mu a}\rho^a, \tag{4.3}$$

where ρ^0 denotes the unit matrix. Note that the first (Greek) index of $\hat{j}_{\mu a}$ refers to the orbital degrees of freedom of the TLS while its second (Latin) index is coupled to the orbital quantum numbers of the electrons. In this simple case the exchange interaction part of the Hamiltonian can be written as

$$H_{\rm exch}=\frac{1}{N}\sum_{\substack{i,\epsilon,\epsilon',m,m',\sigma,\sigma'\\ \mu,a,s,s',\alpha,\alpha'}} j_{\mu a}(b^+_{\alpha s}\tau^\mu_{\alpha\alpha'}S^i_{ss'}b_{\alpha' s'}) \times(a^+_{\epsilon m\sigma}\rho^a_{mm'}\sigma^i_{\sigma\sigma'}a_{\epsilon' m'\sigma'}). \tag{4.4}$$

Substituting the expansion (4.3) of the couplings into Eq. (4.2) we obtain a system of equations for the $\hat{j}_{\mu a}$'s which can be solved exactly (see Appendix B for the details). These equations determine five different fixed manifolds of the scaling equations. However, we have examined the stability of all these fixed manifolds numerically, and we found that they are all unstable except for the one characterized by the equations:

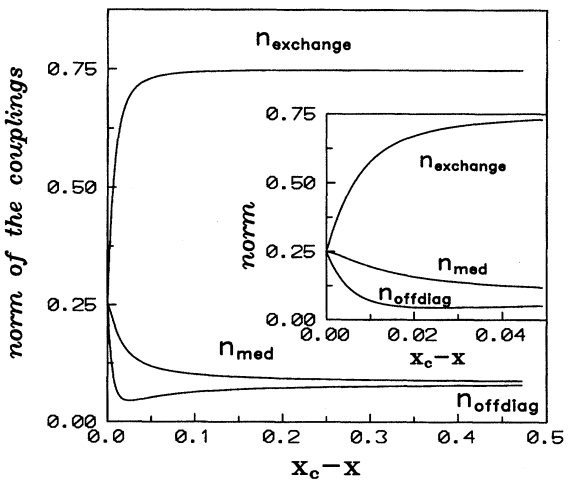

FIG. 2. The scaling of the relative amplitudes $n_{\rm exchange}=j_{00}^2/(\Sigma_{\rho,b=0}^3 j_{\rho a}^2)$, $n_{\rm offdiag}=\Sigma_{a=1}^3 j_{0a}^2/(\Sigma_{\rho,b=0}^3 j_{\rho a}^2)$ and $n_{\rm med}=\Sigma_{\mu,a=1}^3 j_{\mu a}^2/(\Sigma_{\rho,b=0}^3 j_{\rho a}^2)$. The initial couplings $j_{\mu a}(0)$ were generated using Eq. (B13) corresponding to the initial values $n_{\rm exchange}=3/4$ and $n_{\rm med}=n_{\rm offdiag}=1/12$ and then adding small random numbers to them. As one can see from the inset all these relative amplitudes scale to 0.25 as $x\to x_c$ corresponding to the stable fixed point (B12).

$$\hat{j}_{00}=1/4, \quad \hat{j}_{\mu a}=4\hat{j}_{\mu 0}\hat{j}_{0a} \quad (\mu,a=1,\ldots,3),$$
$$\sum_{a=1}^{3}\hat{j}_{0a}^2=\sum_{\mu=1}^{3}\hat{j}_{\mu 0}^2=1/16. \tag{4.5}$$

The result of one of such stability analyses is shown in Fig. 2. In Fig. 2 we investigate the stability of the fixed points determined by Eqs. (B12) and (B13) of Appendix B by first generating the initial couplings $\hat{j}_{\mu a}$ according to Eq. (B13) and then adding small random numbers to them. It can be seen in Fig. 2 that this fixed point is unstable and the normalized exchange coupling $j_{00}^2/(\Sigma_{\mu,a=0}^3 j_{\mu a}^2)$ and the sums $(\Sigma_{a=1}^3 j_{0a}^2)/(\Sigma_{\mu,a=0}^3 j_{\mu a}^2)$ and $(\Sigma_{\mu,a=1}^3 j_{\mu a}^2)/(\Sigma_{\mu,a=0}^3 j_{\mu a}^2)$ scale to the values corresponding to the stable fixed point (B12).

Similarly to Sec. III, due to the special structure (4.5) of the couplings at the stable fixed point the couplings $j_{\mu a}$ factorize, $j_{\mu a}\sim j_{\mu 0}j_{0a}$ $(\mu,a=0.3)$, and we can perform a unitary transformation in the Hilbert space corresponding to the orbital quantum numbers of the electrons and the HP to obtain the following form for the most divergent part of the effective interaction:

$$H_{\rm int}^{\rm eff}(D)\sim\left[\ln\left(\frac{D}{T_K}\right)\right]^{-1}$$
$$\times\sum_{\substack{i,\epsilon,\epsilon',m,m',\sigma,\sigma'\\ s,s',\alpha,\alpha'}}[b_{\alpha s}^{+}(1+\tau^3)_{\alpha\alpha'}S_{ss'}^{i}b_{\alpha' s'}]$$
$$\times[a_{\epsilon m\sigma}^{+}(1+\rho^3)_{mm'}\sigma_{\sigma\sigma'}^{i}a_{\epsilon' m'\sigma'}]. \tag{4.6}$$

The coupling constants $\underline{u}_\mu$ generated by the $\underline{j}_\mu$'s also diverge, as one approaches the Kondo temperature, but for $T_K^{\rm magn}>T_K^{\rm orb}$ their divergence is much slower than that of the $\underline{j}_\mu$'s. This is shown in Fig. 3, where the scaling of the norms $||j||=(\Sigma_{\mu a}j_{\mu a}^2)^{1/2}$ and $||u||=(\Sigma_{\mu a}u_{\mu a}^2)^{1/2}$ of the couplings $j_{\mu a}$ and $u_{\mu a}$ is shown in a logarithmic scale [the couplings $u_{\mu a}$ are defined similarly to the $j_{\mu a}$'s in Eq. (4.3)]. The slow divergence of $||u||$ is due to the special structure of the fixed point. The divergence of the $\underline{u}_\mu$'s is generated by the divergence of the commutator $[\underline{j}_\mu,\underline{j}_\nu]$ on the right-hand side of Eq. (2.8). The most divergent part of the operator $\underline{j}_\mu$ is proportional to $(x-x_c)^{-1}$. However, because of the special structure (4.5) of the stable fixed point the commutator of the most divergent operators, i.e., the term proportional to $\sim(x-x_c)^{-2}$ vanishes in the scaling equation of $\underline{u}_\mu$ and only the products of some less divergent and a most divergent operator give contributions, which explains the slow divergence of $\underline{u}_\mu$. Additionally, since the divergence of the $\underline{u}_\mu$'s is much slower than that of the $\underline{j}_\mu$'s the second term in Eq. (2.10) gives only a negligible contribution to the first term, and therefore, for $T_K^{\rm magn}>T_K^{\rm orb}$ the scaling of the $\underline{j}_\mu$'s isasymptotically decoupled from the scaling of the $\underline{u}_\mu$'s. These numerical results justify the approximation of dropping the second term in Eq. (2.10).

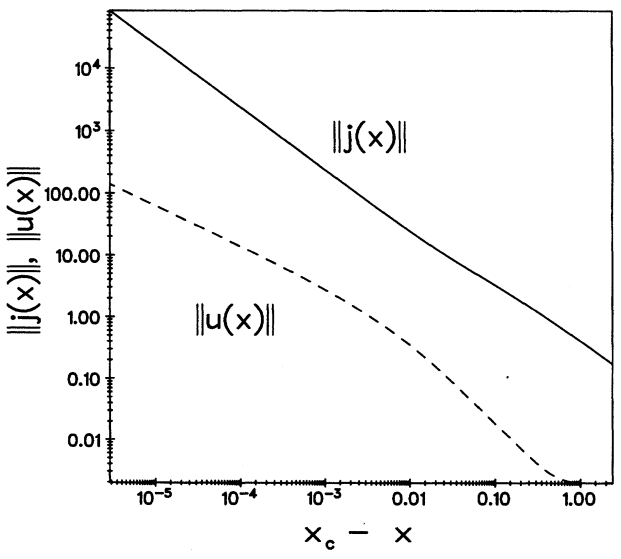

FIG. 3. The scaling trajectory of the norms $||u||=(\Sigma_{\mu,a}u_{\mu a}^2)^{1/2}$ and $||j||=(\Sigma_{\mu,a}j_{\mu a}^2)^{1/2}$ on a logarithmic scale. The initial couplings $j_{\mu a}(0)$ were generated similarly to those of Fig. 2 while the $u_{\mu a}(0)$'s were chosen to be small random numbers. The norm $||u||$ is also diverging as $x\to x_c$ but much slower than that of the exchange coupling $||j||$.

Similarly to the one-channel case the interaction term is different from zero only if the TLS is in the state $\tau^3=+1$. Therefore, in order to form a ground state with energy $\sim T_K$ the orbital motion of the HP must be frozen in. We remark at this point again that the state $\tau^3=+1$ is usually not identical to either the right-hand side or the antisymmetrical state of the HP since a rotation has been performed in the Hilbert space. Furthermore, the projector $1+\rho^3$ implies that only one electron channel is interacting with the TLS. Thus, well below the Kondo temperature, T_K, the HP is frozen into the state $\tau^3=+1$, the Hamiltonian becomes equivalent to the one channel Kondo Hamiltonian and a Fermi-liquid behavior is expected.

Numerical calculations for the case of three orbital channels indicate that for $T_K^{\rm magn}>T_K^{\rm orb}$ the same is going to happen independently of the number of channels considered. Since it is practically impossible to determine all the fixed points for more than two orbital channels we have rather generated some initial couplings corresponding to the physical situation using the simple estimates of Appendix A. To avoid some unrealistic behavior coming from the special symmetries of the oversimplified model used in Appendix A we added to the couplings $\underline{j}_\mu$ small random Hermitian matrices.

Our analysis shows that, similarly to the two-orbital-channel case, the orbital degrees of freedom of the TLS and the HP decouple and the asymptotic form of the effective couplings becomes

$$H_{\rm int}^{\rm eff}(D)\sim\sum_{\substack{i,s,s'\\ \epsilon,\epsilon',\sigma,\sigma'}}\left[\ln\left(\frac{D}{T_K}\right)\right]^{-1}(b_s^{+}\hat{j}_\mu\tau^\mu b_{s'})$$
$$\times S_{ss'}^{i}\sigma_{\sigma\sigma'}^{i}(a_{\epsilon\sigma}^{+}Qa_{\epsilon'\sigma'}), \tag{4.7}$$

where the operator Q is a one-dimensional projector in the orbital quantum numbers of the conduction electrons and the constants $\hat{j}_\mu$'s satisfy

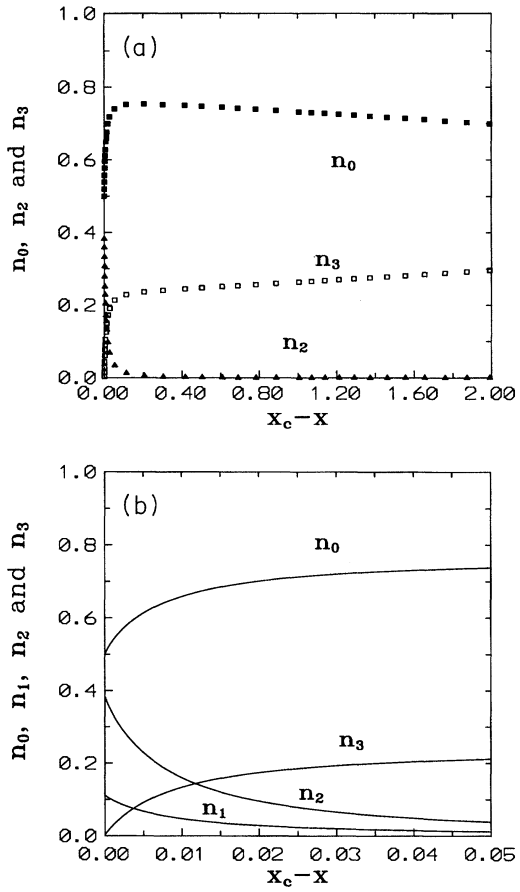

FIG. 4. The scaling of the relative amplitudes $n_\mu = ||\underline{j}_\mu||/(\Sigma||\underline{j}_\nu||)$ of the coupling constants $\underline{j}_\mu$ in the case of three orbital channels. [To assure the transparency of the figure we omitted the trajectory of n_1 in (a).] The initial couplings, $\underline{j}_\mu(0)$, were generated using the equations of Appendix A and adding small Hermitian matrices to them. The dimensionless parameters were chosen to be $k_F a = 0.13$, $\rho_0 J = 0.2$, and $\gamma = 10^{-3}\alpha$. For these parameters the Kondo scale was $x_c = 2.117$. As one can check in (b) that n_0 approaches the value 1/2 at the fixed point and thus the sum rule (4.8) is really satisfied.

$$(\hat{j}_0)^2 = \sum_{\mu=1}^{3} (\hat{j}_\mu)^2 = 1/2. \tag{4.8}$$

This constraint is equivalent to the one that the operator $P = \Sigma \hat{j}_\mu \tau^\mu$ be a one-dimensional projector. Thus the fixed point interaction can be written in the form $H_{\rm int}^{\rm eff}(D) \sim PQS^i\sigma^i$, where the operators P and Q are one-dimensional projectors in the orbital quantum numbers of the TLS and the conduction electrons, respectively.

The asymptotic behavior (4.7) of the scaling equations is illustrated in Fig. 4, where the scaling of the relative amplitude of the different coupling constants $n_\mu(x) = j_\mu^2/\Sigma_\nu j_\nu^2$ is shown, the norms j_μ of the matrices $\underline{j}_\mu$ being defined in the standard way

$$j_\mu = ||\underline{j}_\mu|| = \sqrt{\mathrm{Tr}\{\underline{j}_\mu \underline{j}_\mu\}}. \tag{4.9}$$

One can see in Fig. 4(b) that the n_μ's satisfy the condition (4.8) at the critical value of the scaling parameter, $x_c = \ln(D_0/T_K)$, and n_0 approaches the value 1/2 as $x \to x_c$. We have also checked numerically that all the $\underline{j}_\mu$'s are proportional to the same projector Q at the stable fixed point. Our calculations show as well that the projector Q is mainly projecting out the orbital channel $l = 0$, and the other channels with higher angular momenta give a much smaller contribution to Q.

Since we have obtained the same fixed point structure for both two and three orbital channels we expect that the form (4.7) of the most divergent part of the scaled interaction is very general and holds for any number of orbital channels.

Now we turn to the investigation of the strong orbital interaction limit, $T_K^{\rm orb} > T_K^{\rm magn}$. In this case reaching the orbital Kondo temperature, $T \sim T_K^{\rm orb}$, first an orbital Kondo effect takes place and an orbital singlet state starts to build up. It is obvious from Eq. (2.10) that the orbital Kondo effect generates the exchange couplings as well. In Fig. 5 we show the scaling of the relative weights $||u||/(||u||+||j||)$ and $||j||/(||u||+||j||)$ of the couplings $\underline{u}_\mu$ and $\underline{j}_\mu$ in a logarithmic scale. The initial couplings have been generated using Eq. (A7) of Appendix A.

As one can see, for $J\rho_0 = 0.2$ and $U\rho_0 = 1$ the $\underline{u}_\mu$'s generate the exchange couplings, which become dominating at the Kondo temperature and suppress the effect of the $\underline{u}_\mu$'s [Fig. 5(a)]. On the other hand, for $J\rho_0 = 0.1$ and $U\rho_0 = 1$ both couplings appear to diverge with the same power and their relative weight tends to a constant [see Fig. 5(b)]. According to our numerical calculations the ratio $||j||/||u||$ at the fixed point is universal for $J\rho_0 \ll U\rho_0$. These results indicate that in the latter case a ground state of different physical nature may be formed. This change of the nature of the ground state is slightly indicated in the results of the NRG calculations as well,[38] where the switching on of the initial couplings $\underline{u}_\mu$ resulted in the compression of the lowest lying excited states into well-separated groups.

Analyzing the results of our numerical calculations we found that approaching the fixed point two orbital channels become dominant and the orbital part of the interaction at the fixed point is unitary equivalent with a simple orbital exchange interaction. Thus the fixed point Hamiltonian can be written as

$$H_{\rm int}^{\rm eff} \sim \left[\sum_{i=1}^{3} \sigma^i S^i + \frac{1}{\sqrt{3}} \left(\sum_{i=1}^{3} \sigma^i S^i \right) \left(\sum_{j=1}^{3} \tau^j \rho^j \right) + \frac{1}{2} \sum_{j=1}^{3} \tau^j \rho^j \right]. \tag{4.10}$$

The most interesting feature of this fixed point Hamiltonian is that it is completely symmetrical with respect to the magnetic and orbital degrees of freedom (note that S^i is a spin operator and not a Pauli matrix).

In order to identify the fixed point found we analyzed a simplified model[33] where only interaction terms occurring in Eq. (4.10) are kept:

$$H_{\rm int} = 2J\sigma^i(0)S^i + U\rho^i(0)\tau^i + 2K\sigma^i(0)S^i\rho^j(0)\tau^j. \tag{4.11}$$

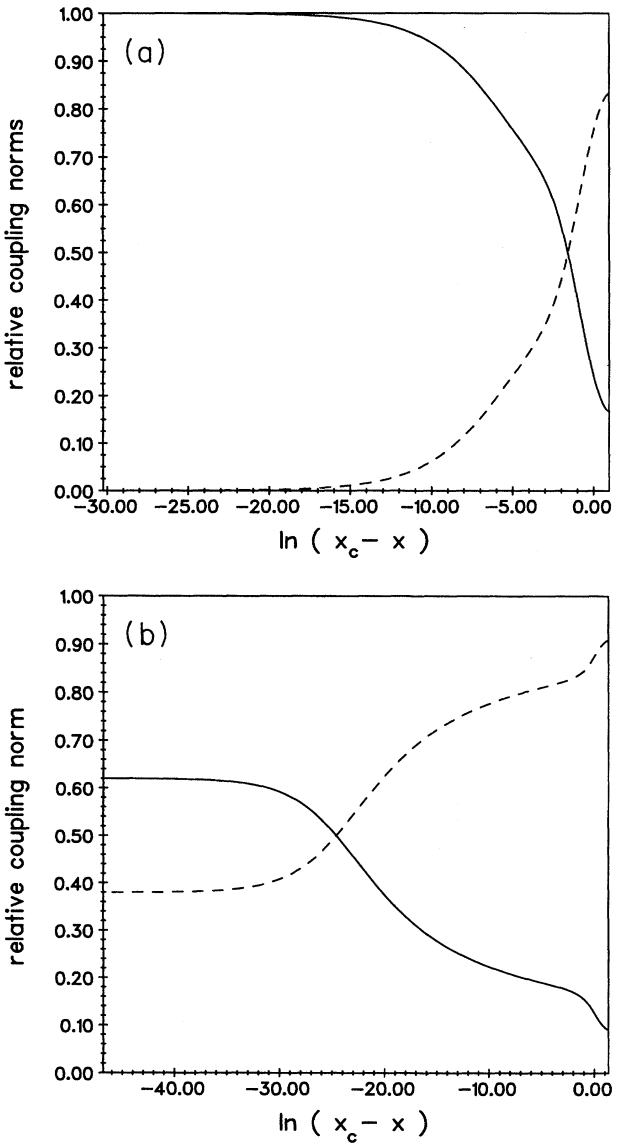

FIG. 5. The scaling trajectory of the relative norms $||u||/(||j||+||u||)$ (dashed line) and $||j||/(||j||+||u||)$ (solid line) in a logarithmic scale. In (a) we have chosen $\rho_0 J=0.2$ and $\rho_0 U=1$ to calculate the initial couplings, while in (b) the values $\rho_0 J=0.1$ and $\rho_0 U=1$ have been used. As one can see, for the small exchange coupling case a different fixed point appears, which, according to the numerical simulations, is characterized by a universal ratio $||j||/||u||$.

Here $\sigma^i(0)$ and $\rho^i(0)$ denote the local spin and orbital pseudospin densities of the conduction electrons and a summation must be carried out over the repeated indices. It is important to note that in this model — in contrast to the interaction term in Eq. (2.4) — the orbital and spin degrees of freedom play equivalent roles. Therefore the Fermi-liquid fixed point (4.7) lies out of the scope of this simplified model which is only adequate to examine the fixed point (4.10).

Then the next to leading logarithmic equations of this simplified model can be generated from the third order vertex corrections and the second order pseudofermion self energy in the standard way:[30]

TABLE I. Relative weights of the singular parts of the scaled interaction operators in Eq. (4.11) at the different fps and their stability in the leading and the next to leading logarithmic orders.

	$\hat{u}$	$\hat{j}$	$\hat{k}$	Leading log stability	Next to leading log stability
(*a*)	0	0	0	Unstable	Unstable
(*b*)	1/4	0	0	Unstable	Unstable
(*c*)	0	1/4	0	Unstable	Unstable
(*d*)	1/4	1/4	0	Unstable	Stable
(*e*)	1/8	1/8	$1/8\sqrt{3}$	Stable	—
(*f*)	$\hat{j}+\hat{u}=1/4$		$\sqrt{\hat{u}\hat{j}/3}$	Unstable	—

$$\frac{dj}{dx}=4(1-4j)(3k^2+j^2),$$

$$\frac{du}{dx}=4(1-4u)(3k^2+u^2), \tag{4.12}$$

$$\frac{dk}{dx}=4k[j+u-(2k^2+j^2+u^2)].$$

The leading logarithmic fixed points of Eqs. (4.12) can be determined by dropping the third-order terms and using a similar ansatz as in Eq. (4.1). The resulting fixed points (i.e., the coefficients $\hat{j}$, $\hat{u}$, and $\hat{k}$) and their stability properties are summarized in Table I. As one can see a variety of fixed points exist but only the one corresponding to Eq. (4.10) is stable.

The picture is somewhat changed in the next to leading logarithmic order, where the fixed points are determined by the vanishing of the right-hand sides of Eqs. (4.12). In effect, fixed points (*a*), (*b*), and (*c*) corresponding to the trivial and the two-channel Kondo fixed points remain unstable similarly to the NRG calculations,[33] however, fixed point (*d*) becomes marginally stable and fixed points (*e*) and (*f*) vanish.

The collapsing of the leading logarithmic stable fixed point (*e*) to the next to leading logarithmic fixed point (*d*) and the fact that in the next to leading logarithmic order fixed point (*d*) is only marginally stable against the double tensor operator in Eq. (4.11) indicate that the ratio $j/k=u/k=\sqrt{3}$ should not be taken too seriously in Eq. (4.10). One rather expects that in an exact solution k/j scales to some universal value which cannot be determined perturbatively.

Having made these remarks one can identify the fixed point (4.10) by means of the results of NRG calculations of Pang.[33] These calculations indicate that the Hamiltonian (4.11) has two interesting fixed points: a stable fixed point with $k=j=u\to\infty$ equivalent to the SU(4) Coqblin-Schrieffer model and also a finite fixed point with $j=u=j^*$ and $k=0$. Since the NRG calculations indicate that this latter is unstable,[33,41] we can identify the stable fixed point (4.10) with the SU(4) Coqblin-Schrieffer fixed point, which corresponds to a Fermi-liquid ground state.

V. CONCLUSIONS

In the present paper we investigated the low-temperature properties of a tunneling HP with spin. It is well known that

scattering on a spinless tunneling HP can result in the formation of an orbital state. As it has been discussed in the Introduction the behavior of such a HP at very low temperatures but still above the splitting energy Δ of the TLS is believed to be equivalent to that of the two-channel Kondo model, where the two channels are due to the spin degrees of freedom of the conduction electrons. This twofold spin channel degeneracy results in the appearance of non-Fermi-liquid properties in contrast to the Fermi-liquid properties of the one-channel Kondo model. If the tunneling particle has a spin as well then the situation becomes different. In this case the $s-d$ scattering on the HP mixes the two channels together, and the original SU(2) symmetry of the conduction electron spin is broken in a dynamical way.

To describe the physical properties of a HP with spin we constructed a model, where in addition to the usual potential scattering we assumed an $s-d$ interaction between the conduction electrons and the HP. It has been shown that the $s-d$ scattering term generates additional terms in the Hamiltonian like "exchange assisted tunneling" and "exchange screening." In the "exchange assisted tunneling" process, for instance, a conduction electron is scattered by the TLS with a spin flip process, while the HP is tunneling from one side of the barrier to the other. The amplitudes of these interactions are small compared to the usual $s-d$ interaction at high temperatures, but they are increasing near the Kondo temperature, and finally, they result in the formation of a nontrivial ground state.

After constructing the Hamiltonian we derived the leading logarithmic scaling equations for the model and we examined their solutions. These scaling equations are very asymmetrical with respect to the orbital and spin degrees of freedom. There are essentially two different energy scales entering into the low-temperature physics of the TLS with spin: the orbital and the magnetic Kondo temperatures given by Eq. (1.1) and Eq. (1.2), respectively. Depending on the relationship between them two basically different cases may occur.

For $T_K^{\rm magn} > T_K^{\rm orb}$, first the magnetic Kondo effect takes place. In this case the potential couplings are also generated by the exchange couplings, but they diverge much slower than the exchange couplings. The leading logarithmic scaling equations have several fixed points. Nevertheless, we have shown numerically that the only stable fixed point is the one where the scaled interaction term is proportional to $\sim PQ\sigma^i S^i$, where P and Q are one-dimensional projectors in the space of the orbital quantum numbers of the TLS and the conduction electrons, respectively. This exchange interaction term vanishes if the HP is not in the state $|p\rangle$ projected out by the operator P: $P|p\rangle = |p\rangle$. Therefore, in order to form a magnetic Kondo state with energy $T_K^{\rm magn}$ the HP has to be frozen into the state $|p\rangle$. The state $|p\rangle$ is generally not localized to one of the potential wells but is rather some linear combination of the two states corresponding to the two minima of the double-well potential. The effect of the projection operator Q is to select a single orbital channel. Thus we conclude that the ground state of the model (i.e., the state which is building up in the region $T_K^{\rm magn} > T > \Delta$) is in this case also equivalent to that of the single-channel antiferromagnetic Kondo model and is a Fermi-liquid state. This is in complete agreement with the results of Cragg *et al.*, and Mirtschin and Lloyd.[38,39]

On the other hand, for $T_K^{\rm magn} < T_K^{\rm orb}$ we predict the appearance of a new ground state where both orbital and magnetic correlations are simultaneously present. In this case the assisted tunneling processes have a very important role. Together with the screening term they generate the orbital Kondo effect and sort out two relevant orbital conduction electron channels, which dominate at low temperatures,[10,21] and we find a fixed point structure which is symmetrical with respect to the orbital and magnetic degrees of freedom. Constructing the next to leading logarithmic scaling equations for a simplified model[33] and comparing our results with those of the NRG calculations[33] we concluded that this other fixed point can be identified with the SU(4) Coqblin-Schrieffer model and corresponds to a Fermi-liquid state.

We have to remark at this point that in the first case, $T_K^{\rm magn} > T_K^{\rm orb}$, the "exchange assisted hoppings," $\underline{j}_1$ and $\underline{j}_2$ may be arbitrarily small, since they are generated by $\underline{j}_0$. Therefore we expect that the "localization of the HP" happens for slow TLS's as well, where the tunneling rate Δ is small enough, and even individual jumps can be observed. In this case we expect that logarithmic anomalies appear as the temperature approaches the Kondo temperature, $T \sim T_K^{\rm magn}$, but at the same time the motion of the HP will be blocked by the splitting up of the two orbital pseudospin states of the HP, and no more individual jumps can be observed. We expect similar effects to occur when the HP is moving on a lattice. On the contrary, TLS's with a reasonable orbital Kondo temperature, $T_K^{\rm orb} \sim 1$ K, necessarily have a large tunneling rate.[10]

It is important to note that all the results above were obtained in the framework of the leading logarithmic approximation, which gives correct results only in the case $T \gg T_K$. In the case of the TLS, for instance, the leading logarithmic approximation predicts the divergence of the vertices at the Kondo temperature, while in the reality the coupling constants remain finite. However, calculations for the original TLS model show[10] that the symmetry properties of the fixed point, i.e., the selection of two orbital electron channels and the SU(2) Lie algebra satisfied by the couplings $\underline{u}_\mu$ ($\mu = 1, \ldots, 3$), is correctly predicted. Therefore we think that our predictions concerning the nature of the ground state of the HP with spin are correct as well.

Finally, we discuss the problem of finding an experimental realization of the model. The $T_K^{\rm magn} > T_K^{\rm orb}$ case can only be observed if the exchange interaction between the HP and the conduction electrons is strong enough. Naturally, for HP's with a nonelectronic spin the exchange interaction with the conduction electrons is too small, thus for $T_K^{\rm magn} > T_K^{\rm orb}$ the only possible candidates are HP's with electronic spin, like magnetic impurities or heavy electrons.

In the opposite — and possibly more interesting — case, $T_K^{\rm magn} > T_K^{\rm orb}$, one not necessarily needs a very strong exchange coupling. As one can see from Eq. (2.10) the exchange couplings are always generated as the orbital Kondo effect occurs, thus the magnetic Kondo effect may be induced even if the exchange interaction is originally small.

The most accurate and convincing measurements of TLS's were performed using metallic nanobridges,[2,14] where

the TLS's are formed in the amorphous region near the orifice. However, this system is probably not adequate for the observation of the phenomena predicted. The most important difficulty is that in order to keep the RKKY interaction small the concentration of magnetic impurities must be small. Therefore the probability of having a tunneling center (TC) with spin is much smaller than that of having a TC without spin corresponding to the ratio of the concentrations. Thus one should perform thousands of experiments in order to observe a single TC with spin. Additionally, the microscopic origin of the TC's in these nanostrictions is still unclear.

More promising candidates are alloys like $Pb_{1-x}Ge_xTe$.[8] In this alloy the diameter of the Ge^{2+} ions is considerably smaller than that of the Pb^{2+} ions and they can form octopole centers. For small enough Ge concentrations logarithmic resistivity anomalies have been observed which were interpreted in terms of the orbital Kondo effect due to the TC's.[8,42]

Substituting the Ge^{2+} ions by some suitably chosen magnetic impurity (Fe^{2+}, for example) one could produce magnetic TC's with $T_K^{\rm orb} > T_K^{\rm magn}$ in a controlled way. However, in order to reach the region $T_K^{\rm magn} > T_K^{\rm orb}$ one should increase the number of charge carriers, which is difficult. However, in a similar metallic system it might be possible to tune the orbital Kondo temperature with respect to the magnetic Kondo temperature by applying a stress on the material, and the blocking of the tunneling centers might be seen in ultrasound measurements.[9] One could also imagine to observe individual tunneling centers in these materials by performing STM measurements.

ACKNOWLEDGMENTS

The author is especially grateful to A. Zawadowski for helpful discussions and his careful reading of the manuscript. He would also like to thank H. Pang for his valuable remarks. This research has been supported by Hungarian Grants Nos. OTKA 7283/93 and OTKA F016604.

APPENDIX A: ESTIMATION OF THE INITIAL COUPLINGS

In this appendix we estimate the different initial coupling constants $\underline{j}_\mu$ and $\underline{u}_\mu$. For the sake of simplicity we assume that the $s-d$ and the potential scattering is local, i.e.,

$$J(\mathbf{r}-\mathbf{R}) = J\,\delta(\mathbf{r}-\mathbf{R}),$$
$$U(\mathbf{r}-\mathbf{R}) = U\,\delta(\mathbf{r}-\mathbf{R}). \tag{A1}$$

We also assume a free electron gas with a spherical Fermi surface and Fermi momentum k_F, and a symmetrical double-well potential with cylindrical symmetry. In this case the dimensionless coupling constants $j^\mu_{\mathbf{k}\mathbf{k}'} = \rho_0 J^\mu_{\mathbf{k}\mathbf{k}'}$ and $u^\mu_{\mathbf{k}\mathbf{k}'} = \rho_0 U^\mu_{\mathbf{k}\mathbf{k}'}$ can be written as

$$j^\mu_{\mathbf{k}\mathbf{k}'} = (\rho_0 J) A^\mu_{\mathbf{k}\mathbf{k}'}, \quad u^\mu_{\mathbf{k}\mathbf{k}'} = (\rho_0 U) A^\mu_{\mathbf{k}\mathbf{k}'}, \tag{A2}$$

where the matrix elements $A^\mu_{\mathbf{k}\mathbf{k}'}$ characteristic to the TLS are given by

$$A^\mu_{\mathbf{k}\mathbf{k}'} = \frac{1}{2}\sum_{\alpha,\beta} \tau^\mu_{\beta\alpha} \int d^3\mathbf{r} e^{i(\mathbf{k}'-\mathbf{k})\mathbf{r}} \varphi^*_\alpha(\mathbf{r})\varphi_\beta(\mathbf{r}), \tag{A3}$$

the φ_α's ($\alpha = \pm 1$) being the left- and right-hand side wave functions of the HP, respectively. The integral in Eq. (A3) can be developed with respect to $k_F d$, d being the distance between the two minima of the potential well.[10] Since we have a spherical Fermi surface it is worth choosing the orthogonal set of wave functions $\{f_n\}$ to be proportional to the spherical functions $Y_{lm}(\vartheta,\varphi)$, where corresponding to the symmetry of the problem the axis z is chosen to coincide with the symmetry axis of the double well potential.

Up to second order in $k_F d$ we obtain the following expressions for the $\underline{A}_\mu$'s:

$$\underline{A}_0 = \begin{pmatrix} 1-\beta & 0 & -\beta/\sqrt{5} \\ 0 & \beta & 0 \\ -\beta/\sqrt{5} & 0 & 0 \end{pmatrix},$$
$$\underline{A}_1 = \begin{pmatrix} -\gamma & 0 & -\gamma/\sqrt{5} \\ 0 & \gamma & 0 \\ -\gamma/\sqrt{5} & 0 & 0 \end{pmatrix},$$
$$\underline{A}_2 = 0, \tag{A4}$$
$$\underline{A}_3 = \begin{pmatrix} 0 & -i\alpha & 0 \\ i\alpha & 0 & 0 \\ 0 & 0 & 0 \end{pmatrix},$$

where the $\underline{A}_\mu$'s are defined like the $\underline{j}_\mu$'s in Eqs. (2.9) and (2.10), and the indices 1,2,3 of the matrices refer to the orbital channels $(l,m) = (0,0)$, $(1,0)$, and $(2,0)$. The constants α, β, and γ are given by the following expressions:

$$\alpha = \frac{4\pi}{\sqrt{3}} k_F \int d^3\mathbf{r} (\hat{d}\mathbf{r}) \varphi^*_r(\mathbf{r})\varphi_r(\mathbf{r}),$$
$$\beta = \frac{4\pi}{3} k_F^2 \int d^3\mathbf{r} (\hat{d}\mathbf{r})^2 \varphi^*_r(\mathbf{r})\varphi_r(\mathbf{r}), \tag{A5}$$
$$\gamma = \frac{4\pi}{3} k_F^2 \int d^3\mathbf{r} (\hat{d}\mathbf{r})^2 \varphi^*_r(\mathbf{r})\varphi_l(\mathbf{r}),$$

where the states φ_r and φ_l are localized in the right and left minima of the double-well potential, respectively, and $\hat{d}$ is a unit vector parallel to the axis of the TLS. Assuming a quasi-one-dimensional motion of the HP one can give a rough estimation for the integrals in Eq. (A.5):[10] $\alpha \approx (k_F d) 2\pi/\sqrt{3}$, $\beta \approx (k_F d)^2 \pi/3$, and $\gamma \approx 10^{-3}\alpha$. One can also express the initial couplings $j_\mu(0)$ and $j_{\mu a}(0)$ in terms of the constants α, β, and γ. Projecting out the channel $l=0$, which has the largest scattering amplitude we obtain

$$j_\mu(0) = (\rho_0 J)(1-\beta, -\gamma, 0, 0), \tag{A6}$$

while the matrix $j_{\mu a}(0)$ can be estimated by projecting out the $l=0,1$ channels:

$$j_{\mu a}(0)=(\rho_0 J)\begin{pmatrix} \frac{1}{2} & 0 & 0 & \frac{1}{2}-\beta \\ 0 & 0 & 0 & -\gamma \\ 0 & 0 & 0 & 0 \\ 0 & 0 & \alpha & 0 \end{pmatrix} . \tag{A7}$$

The initial value $u_{\mu a}(0)$ of the matrix $u_{\mu a}$ is given by a similar formula.

APPENDIX B: EXAMINATION OF THE FIXED POINT STRUCTURE OF THE LEADING LOGARITHMIC SCALING EQUATIONS FOR A TUNNELING HP WITH SPIN

To obtain the asymptotic structure of exchange couplings we substitute the expansion of the couplings $\hat{j}_\mu$ in Eq. (4.3) into Eq. (4.2) to get

$$\hat{j}_{\mu 0}=2\sum_{b=0}^{3}\hat{j}_{\mu b}\hat{j}_{0b}, \tag{B1}$$

$$\hat{j}_{\mu a}=2(\hat{j}_{00}\hat{j}_{\mu a}+\hat{j}_{0a}\hat{j}_{\mu 0}), \tag{B2}$$

$$\hat{j}_{00}=\sum_{\rho,b=0}^{3}\hat{j}_{\rho b}\hat{j}_{\rho b}, \tag{B3}$$

$$\hat{j}_{0a}=2\sum_{\rho=0}^{3}\hat{j}_{\rho a}\hat{j}_{\rho 0}, \tag{B4}$$

where the indices μ and a take the values $\mu,a=1,\ldots,3$. Equivalently, we can write Eq. (B2) in the form

$$(\tfrac{1}{2}-\hat{j}_{00})\hat{j}_{\mu a}=\hat{j}_{0a}\hat{j}_{\mu 0} \quad (\mu,a=1,\ldots,3). \tag{B5}$$

Substituting this equation into Eqs. (B1) and (B4) we obtain the following equations:

$$(\tfrac{1}{2}-\hat{j}_{00})^2\hat{j}_{\mu 0}=\left(\sum_{a=1}^{3}\hat{j}_{0a}^2\right)\hat{j}_{\mu 0} \quad (\mu=1,\ldots,3), \tag{B6}$$

$$(\tfrac{1}{2}-\hat{j}_{00})^2\hat{j}_{0a}=\left(\sum_{\mu=1}^{3}\hat{j}_{\mu 0}^2\right)\hat{j}_{0a} \quad (a=1,\ldots,3). \tag{B7}$$

At this point two different cases may occur.

Case A: $\hat{j}_{00}=1/2$. In this case Eqs. (B6) and (B7) tell us that either $\hat{j}_{0a}\equiv 0$ for $(a=1,\ldots,3)$ or $\hat{j}_{\mu 0}\equiv 0$ for $(\mu=1,\ldots,3)$. If $\hat{j}_{0a}\equiv 0$ then $\hat{j}_{\mu 0}$ and $\hat{j}_{\mu a}$ must satisfy the equations

$$\begin{gathered}\sum_{\mu=1}^{3}\hat{j}_{\mu a}\hat{j}_{\mu 0}=0 \quad (a=1,\ldots,3), \\ \sum_{\mu,a=1}^{3}\hat{j}_{\mu a}^2+\sum_{\mu=1}^{3}\hat{j}_{\mu 0}^2=\frac{1}{4},\end{gathered} \tag{B8}$$

while in the other case, $\hat{j}_{\mu 0}\equiv 0$, the following constraints must be satisfied:

$$\begin{gathered}\sum_{a=1}^{3}\hat{j}_{\mu a}\hat{j}_{0a}=0 \quad (\mu=1,\ldots,3), \\ \sum_{\mu,a=1}^{3}\hat{j}_{\mu a}^2+\sum_{a=1}^{3}\hat{j}_{0a}^2=\frac{1}{4}.\end{gathered} \tag{B9}$$

Thus, for $\hat{j}_{00}=1/2$ we have two different fixed point structures, determined by Eqs. (B8) and (B9).

Case B: $\hat{j}_{00}\neq 1/2$. If $\hat{j}_{0a}\equiv 0$ for $(a=1,\ldots,3)$ or $\hat{j}_{\mu 0}\equiv 0$ for $(\mu=1,\ldots,3)$ then it is obvious from Eqs. (B2), (B6), and (B7) that all the couplings $\hat{j}_{\mu a}$ vanish except for $\hat{j}_{00}$:

$$\hat{j}_{\mu a}=\delta_{\mu,0}\delta_{a,0}\hat{j}_{00} . \tag{B10}$$

This fixed point is the trivial Kondo fixed point which has been shown to be unstable in Sec. III.

If there is a value of $\mu\neq 0$ for which $j_{\mu 0}\neq 0$ then we can express $\Sigma_{\mu,a=1}^{3}\hat{j}_{\mu a}^2$, $\Sigma_{a=1}^{3}\hat{j}_{0a}^2$, and $\Sigma_{\mu=1}^{3}\hat{j}_{\mu 0}^2$ from Eqs. (B5), (B6), and (B7), and substitute into Eq. (B3). This gives a second-order equation for $\hat{j}_{00}$ with the roots

$$\hat{j}_{00}=\frac{1}{2}\pm\frac{1}{4} . \tag{B11}$$

The root $\hat{j}_{00}=1/4$ corresponds to the fixed point

$$\begin{gathered}\sum_{\mu=1}^{3}\hat{j}_{\mu 0}^2=\sum_{a=1}^{3}\hat{j}_{0a}^2=\frac{1}{16}, \\ \hat{j}_{\mu a}=4\hat{j}_{\mu 0}\hat{j}_{0a} \quad (\mu,a=1,\ldots,3),\end{gathered} \tag{B12}$$

while the other root, $\hat{j}_{00}=3/4$, determines the fixed point

$$\begin{gathered}\sum_{\mu=1}^{3}\hat{j}_{\mu 0}^2=\sum_{a=1}^{3}\hat{j}_{0a}^2=\frac{1}{16}, \\ \hat{j}_{\mu a}=-4\hat{j}_{\mu 0}\hat{j}_{0a} \quad (\mu,a=1,\ldots,3).\end{gathered} \tag{B13}$$

Numerical investigations of the scaling equations show that the fixed points corresponding to Eqs. (B8), (B9), (B10), and (B13) are unstable, and that in the case of two orbital channels the only stable fixed point is given by Eq. (B12). At this fixed point the orbital degrees of freedom of the TLS and the conduction electrons factorize, and the fixed point coupling becomes of the form

$$H_{\rm int}^{\rm eff}\sim\hat{j}_{\mu a}\tau^\mu\rho^a\sim(a_\mu\tau^\mu)(b_a\rho^a), \tag{B14}$$

where the four-vectors a_μ and b_a satisfy the equations

$$a_0^2=\sum_{\mu=1}^{3}a_\mu^2, \quad b_0^2=\sum_{a=1}^{3}b_a^2, \tag{B15}$$

i.e., the operators $P=\Sigma a_\mu\tau^\mu$ and $Q=\Sigma b_a\rho^a$ are one-dimensional projectors.

[1] For a review see J. L. Black, in *Metallic Glasses*, edited by H. J. Güntherodt and H. Beck (Springer, New York, 1981).
[2] K. S. Ralls and R. A. Buhrman, Phys. Rev. Lett. **60**, 2434 (1988); Phys. Rev. B **44**, 5800 (1991).
[3] N. Giordano, in *Quantum Tunneling in Condensed Media*, edited by Yu. Kagan and A. J. Leggett (North-Holland, Amsterdam, 1992).
[4] J. Kondo, Physica B (Amsterdam) **84**, 40 (1976).
[5] A. Zawadowski, Phys. Rev. Lett. **45**, 211 (1980).
[6] D. C. Ralph and R. A. Buhrman, Phys. Rev. Lett. **69**, 2118 (1992).
[7] T. Ishiguro *et al.*, Phys. Rev. Lett. **69**, 660 (1993).
[8] S. Katayama, S. Maekawa, and H. Fukuyama, J. Phys. Soc. Jpn. **50**, 694 (1987); S. Takano, Y. Kumashiro, and K. Tsuji, *ibid.* **53**, 4309 (1984).
[9] A. K. Raychaudhuri and S. Hunklinger, Z. Phys. B **57**, 113 (1984).
[10] K. Vladár and A. Zawadowski, Phys. Rev. B **28**, 1564 (1983); **28**, 1582 (1983); **28**, 1596 (1983).
[11] V. Hakim, A Muramatsu, and F. Guinea, Phys. Rev. B **30**, 464 (1984).
[12] A. J. Leggett *et al.*, Rev. Mod. Phys. **59**, 1 (1987).
[13] Yu. Kagan and N. V. Prokof'ev, in *Quantum Tunneling in Condensed Media*, edited by Yu. Kagan and A. J. Leggett (North-Holland, Amsterdam, 1992).
[14] N. M. Zimmerman, B. Golding, and W. H. Haemmerle, Phys. Rev. Lett. **67**, 1322 (1991); B. Golding, N. M. Zimmerman, and S. N. Coppersmith, *ibid.* **68**, 998 (1992).
[15] D. H. Cobden, M. J. Uren, and M. Pepper, Phys. Rev. Lett. **71**, 4230 (1993).
[16] K. Vladár, G. Zimányi, and A. Zawadowski, Phys. Rev. Lett. **56**, 286 (1986); K. Vladár, A. Zawadowski, and G. Zimányi, Phys. Rev. B **37**, 2001 (1988); **37**, 2015 (1988).
[17] K. Vladár, Prog. Theor. Phys. **90**, 43 (1993).
[18] G. Zaránd, Solid State Commun. **86**, 413 (1993); G. Zaránd and A. Zawadowski, Phys. Rev. Lett. **72**, 542 (1994); Phys. Rev. B **50**, 932 (1994).
[19] D. C. Ralph, A. W. W. Ludwig, Jan von Delft, and R. A. Buhrman, Phys. Rev. Lett. **72**, 1064 (1994); D. C. Ralph and R. A. Buhrman, Phys. Rev. B **51**, 3554 (1995).
[20] D. L. Cox and A. E. Ruckenstein, Phys. Rev. Lett. **71**, 1613 (1993); M. H. Hettler, J. Kroha, and S. Hershfield, *ibid.* **73**, 1967 (1994).
[21] G. Zaránd, Phys. Rev. B **51**, 273 (1995).
[22] G. Zaránd and K. Vladár (unpublished).
[23] In this paper we follow the terminology used in the TLS literature. (Refs. 5, 6, 10, 16, 18, and 19). Accordingly, the term "electronic orbital channel" is used for the different angular momentum scattering channels. This should be contrasted to the terminology of the multichannel Kondo model and NRG calculations, where the term "electronic orbital channel" is replaced by "local conduction electron orbitals." The "real spin index," or equivalently, the "flavor index" in the generalized TLS model (Ref. 21), corresponds to the "channel index" in the multichannel Kondo model.
[24] P. B. Wiegemann and A. M. Tsvelik, Pis'ma Zh. Éksp. Teor. Fiz. **38**, 480 (1983) [JETP Lett. **38**, 591 (1983)]; N. Andrei and C. Destri, Phys. Rev. Lett. **52**, 364 (1984); for a review see P. Schlottmann and P. D. Sacramento, Adv. Phys. **42**, 641 (1993).
[25] A. W. W. Ludwig and I. Affleck, Phys. Rev. Lett. **67**, 161 (1991); **67**, 3160 (1991); A. W. W. Ludwig and I. Affleck, *ibid.* **67**, 3160 (1991); I. Affleck and A. W. W. Ludwig, Phys. Rev. B **48**, 16301 (1993).
[26] G. Grüner and A. Zawadowski, Rep. Prog. Phys. **37**, 1500 (1074).
[27] N. Andrei, K. Furuya, and J. H. Lowenstein, Rev. Mod. Phys. **32**, 331 (1983); A. M. Tsvelik and P. B. Wiegmann, Adv. Phys. **32**, 453 (1983).
[28] A. Muramatsu and F. Guinea, Phys. Rev. Lett. **57**, 2337 (1986); for a review see N. E. Bickers, Rev. Mod. Phys. **59**, 845 (1987).
[29] P.W. Anderson, J. Phys. C **3**, 2436 (1970).
[30] M. Fowler and A. Zawadowski, Solid State Commun. **9**, 471 (1971); A. A. Abrikosov and A. A. Migdal, J. Low Temp. Phys. **3**, 519 (1970).
[31] G. Yuval and P. W. Anderson, Phys. Rev. B **1**, 1522 (1970); P. W. Anderson, G. Yuval, and D. R. Hamann, *ibid.* **1**, 4464 (1970).
[32] H. B. Pang and D. L. Cox, Phys. Rev. B **44**, 9454 (1991); I. Affleck, A. W. W. Ludwig, H. B. Pang, and D. L. Cox, *ibid.* **45**, 7918 (1992).
[33] H. B. Pang, Phys. Rev. Lett. **73**, 2736 (1994).
[34] H.B. Pang, Ph.D. dissertation, Ohio State University, 1992.
[35] H. Ishii, J. Low Temp. Phys. **32**, 457 (1978); E. Müller-Hartmann, Z. Phys. **223**, 227 (1969).
[36] P. Nozières, J. Low Temp. Phys. **17**, 31 (1974).
[37] K. Yamada, Prog. Theor. Phys. **53**, 970 (1975); K. Yamada and K. Yoshida, *ibid.* **53**, 1286 (1975).
[38] D. M. Cragg, P. Lloyd, and P. Nozières, J. Phys. C **13**, 803 (1980).
[39] A. W. Mirtschin and P. Lloyd, J. Phys. C **17**, 5399 (1984).
[40] A. A. Abrikosov, Physics **2**, 5 (1965).
[41] H. B. Pang (private communication).
[42] Recent reinvestigations of the experimental results show that in the PbGeTe alloys the orbital Kondo effect is induced by a phonon mediated electron assisted tunneling mechanism, where the interaction between the conduction electrons and the TC's is mediated by a soft optical phonon mode associated with the structural phase transition [G. Zaránd (unpublished)].